Electronic Supplementary Information

Translucent, Hydrophobic, and Mechanically Tough Aerogels Constructed from Trimethylsilylated Chitosan Nanofibers

Satoru Takeshita, and Satoshi Yoda*

Detailed experimental procedure

Materials. Chitosan (deacetylation degree: 79.5%, viscosity: 20–200 mPa s at 5 g L^{-1}; 20 °C), aqueous formaldehyde solution (36.5 wt%), 1,1,1,3,3,3-hexamethyldisilazane (HMDS, 96.0%), acetic acid (99.7%), methanol (99.8%), acetone (99.0%), superdehydrated acetone (99.5%), and ammonia solution (25% aqueous solution) were purchased from Wako Pure Chemical Industries. Tetramethoxysilane (LS-540) was purchased from Shin-Etsu Chemical. Liquid CO_2 (99.9%) was purchased from Iwatani Corporation.

Synthesis of chitosan organogels. Aqueous chitosan solution (6.0 mL, 5 g L^{-1}, 0.5 vol% acetic acid solution) was mixed with aqueous formaldehyde solution (1.5 mL) in a 33.0 mmϕ petri dish and aged at 60 °C overnight in a sealed container. The obtained hydrogel was soaked in methanol under constant stirring at room temperature for at least 2 days with a constant change of methanol and then soaked in acetone for at least 2 days as well. Superdehydrated acetone was used as the final solvent of the gel.

Trimethylsilylation and supercritical drying. The obtained organogel containing acetone was silylated by soaking in HMDS–superdehydrated acetone solution (HMDS 0–25 vol%, 100 mL for one gel) for 24 h at room temperature under constant stirring. After the silylation, the obtained gel was soaked in acetone under constant stirring at room temperature for at least 2 days with a constant change of acetone. Finally, the washed organogel was placed in a stainless autoclave (Taiatsu Techno, TAS-047) with approximately 125 mL of superdehydrated acetone. The temperature and pressure of the autoclave were set to 60 °C and 20 MPa, respectively, by introducing CO_2. After keeping overnight, the solvent was extracted with supercritical CO_2 at 60 °C and 20 MPa for ~12 h. After the extraction, the pressure was slowly reduced to the ambient pressure to give aerogel.

We also prepared trimethylsilylated chitosan xerogel (HMDS 0.5 vol%) by simply drying the washed organogel at 60 °C for 1 h under ambient pressure and confirmed that the washed organogel does not contain any entrapped species, such as unreacted HMDS (Fig. S2).

Preparation of silica aerogel. We prepared conventional silica aerogel for comparison purpose. Tetramethoxysilane, methanol, and 0.001 mol L^{-1} aqueous ammonia solution were mixed at 2:4:1 in volume ratio. This mixture was poured into a Teflon petri dish and aged overnight at room temperature to form a gel. The obtained gel was washed by soaking in methanol at room temperature for 2 days with a constant change of methanol. The washed silica organogel was silylated by soaking in HMDS–methanol solution (HMDS concentration of 10 vol%) at 60 °C for 3 h. After the silylation, the obtained gel was washed again in methanol for 1 day and then placed in a stainless pressure vessel (approximately ~50 mL in volume) with ~20 mL of methanol. The temperature and pressure of the autoclave were set to 80 °C and 20 MPa, respectively, and the solvent was extracted with supercritical CO_2 at 80 °C and 20 MPa, followed by gradual reduction of the pressure to give silica aerogel.

Characterization. The apparent density of aerogel was calculated from the diameter, height, and weight of the aerogel. The Fourier-transform infrared (FT-IR) transmission spectra were measured in pressed KBr disks on a spectrometer (JASCO, FT/IR-660 plus). The solid state cross polarization magic-angle spinning (MAS) NMR spectra were recorded on an NMR instrument (Bruker, AVANCE III 400WB) equipped with a 4 mm MAS probe, operating at 300K, with the MAS speed of 12.5 kHz, and at Larmor frequencies of 79.5 and 100.6 MHz for ^{29}Si and ^{13}C, respectively. The C/N atomic ratio was measured using an elemental analyzer (PerkinElmer 2400) at the combustion and reduction temperatures of 925 and 640 °C, respectively. The water contact angles were measured using an automatic contact angle analyzer (Kyowa Interface Science, DMs-401) with a 1.0 μL water droplet for each measurement. The transmission spectra were measured on a UV–visible spectrometer (JASCO, V-570). The microstructure of aerogel was observed with a field-emission scanning electron microscope (SEM; Hitachi, SU9000). The sample for SEM observation was coated with a thin Pd–Pt conductive layer. The brightness and contrast of SEM images were optimized on PowerPoint 2013. The nitrogen gas sorption isotherms were measured on an automatic gas sorption instrument (MicrotracBel, BELSORP-max) at 77 K. The compression stress–strain curves were recorded on a table-top universal mechanical tester (Shimadzu, EZ Test EZ-LX) equipped with 5 kN load cell at the compression rate of 1.00 mm min^{-1}. The compression elastic modulus was calculated from the slope of the linear part in the 0–25% strain region. Photographs were taken with digital cameras (Canon, SX110 IS; Fujitsu, Arrows F-03H) and their brightness and contrast were optimized on PowerPoint 2013.

The degree of silylation (*DS*) is defined as the ratio of the number of introduced $Si(CH_3)_3$ groups to the number of OH groups. The *DS* values were calculated from C/N atomic ratios based on the following assumptions: (i) NH_2 groups do not participate in the silylation process since almost all of them are already used in the cross-linking reaction with formaldehyde and the degree of cross-linking does not change during the silylation process, (ii) impurities, such as a small amount of

proteins from crab shells, do not participate in the silylation process, and (iii) the increase in C/N ratio of the trimethylsilylated sample compared to that of the unmodified sample is attributed to only introduced $Si(CH_3)_3$ groups. On the basis of above-mentioned assumptions, *DS* is calculated by Equation (S1):

$$DS = [\text{number of } Si(CH_3)_3 \text{ groups}] / [\text{number of OH groups}]$$
$$= [\{(C/N)_{silylated} - (C/N)_{unmodified}\}/3] / 2 \quad \text{(S1)}$$

where $(C/N)_{silylated}$ and $(C/N)_{unmodified}$ are C/N atomic ratios of trimethylsilylated and unmodified samples, respectively.

Additional figures and tables

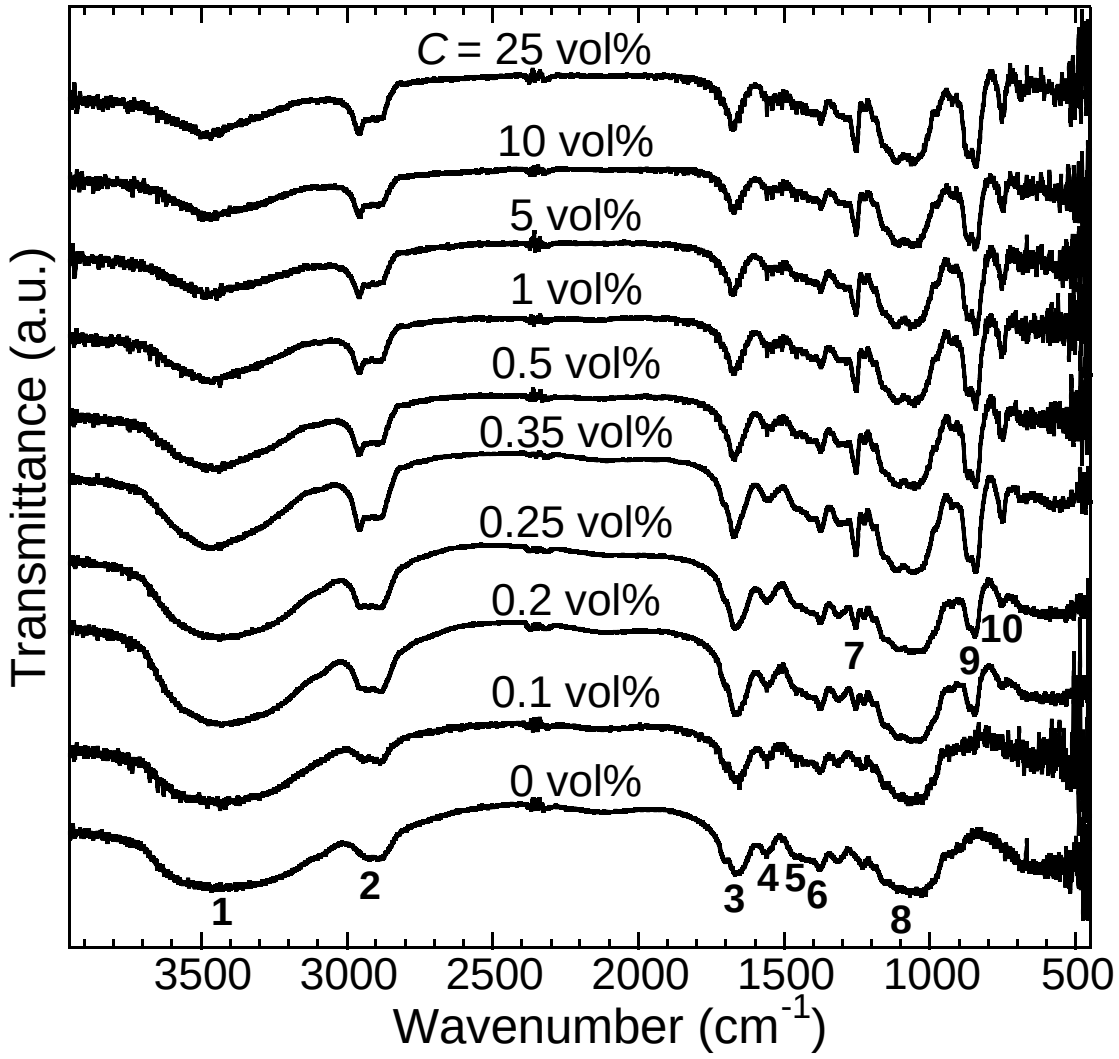

Figure S1. FT-IR spectra of the samples prepared with different HMDS concentrations.

Table S1. Assignments for FT-IR spectra.

Peak	Wavenumber [cm^{-1}]	Assignment	Ref.
1	~3430	O–H stretching, N–H stretching,	[S1,S2]
2	2865–2920	C–H stretching	[S1,S2]
3	~1660	C=O (in *N*-acetylglucosamine units)	[S2]
4–6	1380–1590	CH_2 scissoring/bending/wagging	[S1,S2]
7	1253	Si–C bending	[S3,S4]
8	~1050	C–C, C–N, C–O–C	[S1,S2]
9	843, 867	Si–C stretching	[S3,S4]
10	754	C–H bending in $Si–CH_3$	[S3,S4]

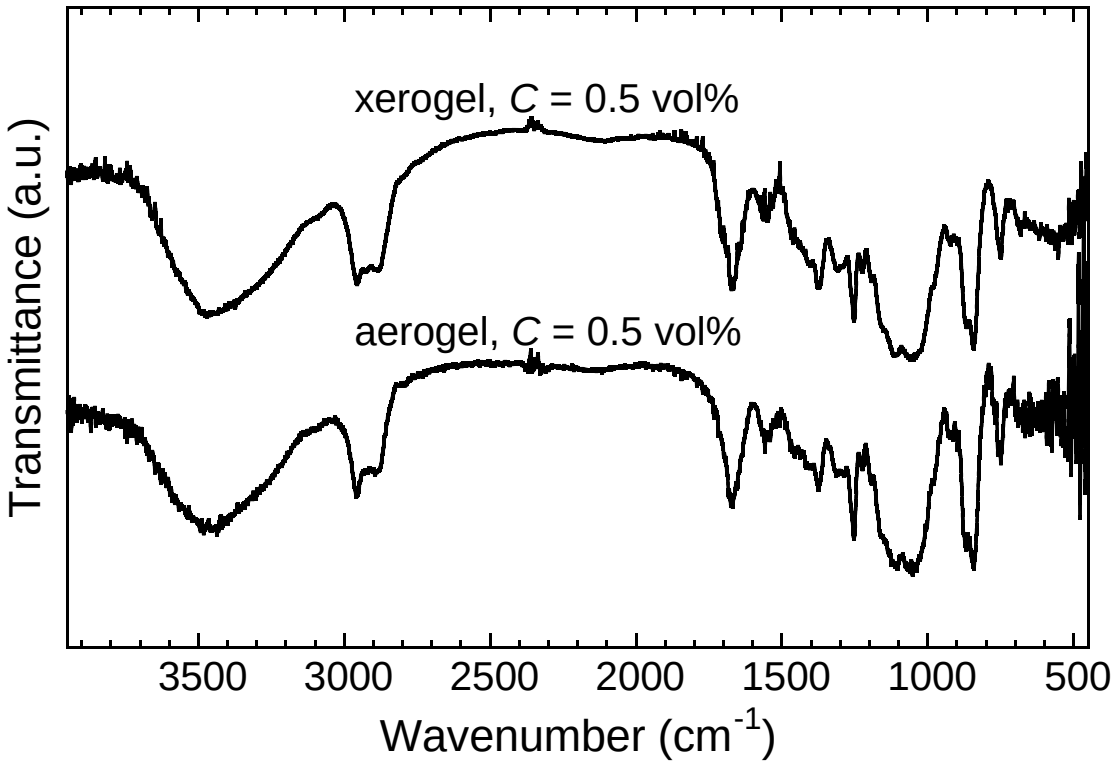

Figure S2. FT-IR spectra of the trimethylsilylated chitosan xerogel and aerogel (*C* = 0.5 vol%). The relative intensity of Si–CH_3 (1253 and ~850 cm^{-1}) is almost the same between xerogel and aerogel, indicating that unreacted and entrapped HMDS does not exist after washing. In addition, the size of the HMDS molecule is less than ~1 nm, which is far smaller than the pore size, ~50 nm. Judging from these items, the residual unreacted HMDS does not significantly affect the nanostructure of the final aerogels.

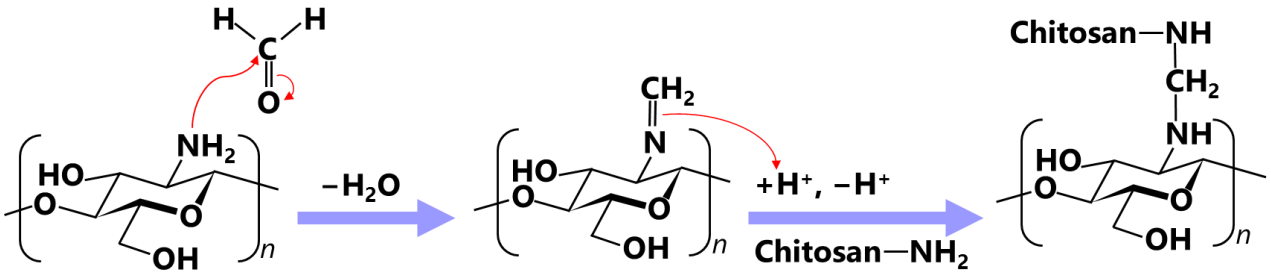

Scheme S1. Proposed reaction mechanism of cross-linking.[S1,S5,S6] The ^{13}C NMR spectrum (the bottom of Fig. 1) contains no signal for $NH{=}CH_2$ around ~160 ppm, showing the instability of intermediate Schiff's base. A small ^{13}C peak at 40–50 ppm is possibly attributed to the methylene bridge of cross-linking bonds.[S7] However, since formaldehyde easily polymerizes in aqueous solution, the possibility of bridging through paraformaldehyde $–(CH_2O)_n–$ species, which is supposed to appear at around 90–100 ppm overlapping with the signals from chitosan chain,[S8] cannot be denied.

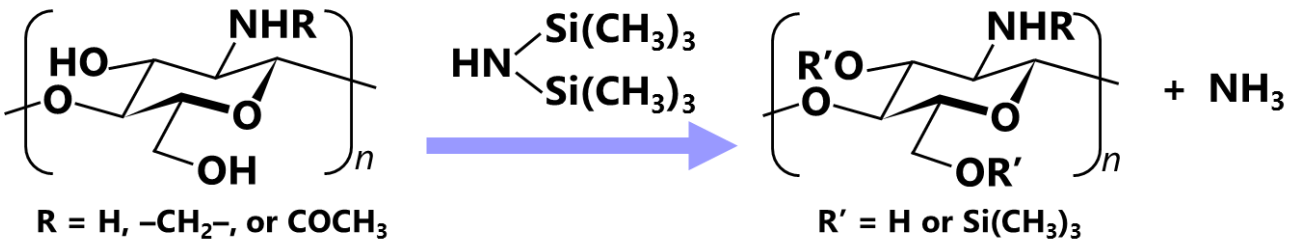

Scheme S2. Proposed reaction scheme for trimethylsilylation.[S9,S10] One HMDS molecule can provide two trimethylsilyl groups and one NH_3.[S9] Since the ^{29}Si NMR spectra (the top of Fig. 1) only contains the signal from –O–**Si**–$(CH_3)_3$ species (~22 ppm), the oxidation of HMDS to form polymerized species such as –O–Si$(CH_3)_2$–O–Si–$(CH_3)_3$ does not occur in our system. The ^{29}Si NMR peak for –O–**Si**–$(CH_3)_3$ and the ^{13}C peak for –O–Si–(**C**$H_3)_3$ (2–3 ppm) show small splits. This might be attributed to the variation of OH groups, such as C3 and C6 positions and chitin/chitosan units. We also note that triacetonamine, which can be formed by condensation between aetone and ammonia derived from HMDS during silylation, is not detected by IR or NMR spectroscopies probably because they are removed through washing procedure.

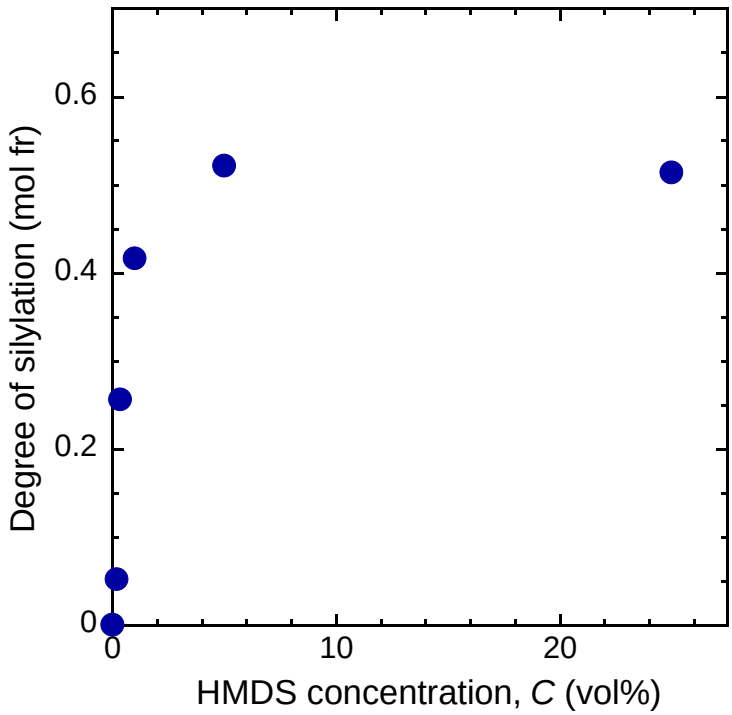

Figure S3. Change in degree of silylation of chitosan aerogels with HMDS concentration.

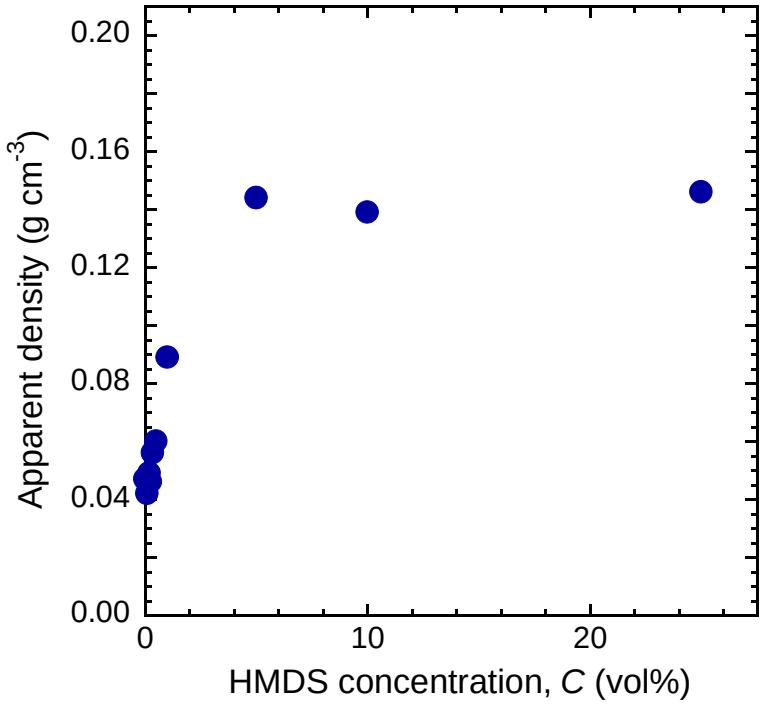

Figure S4. Change in apparent density of chitosan aerogels with HMDS concentration.

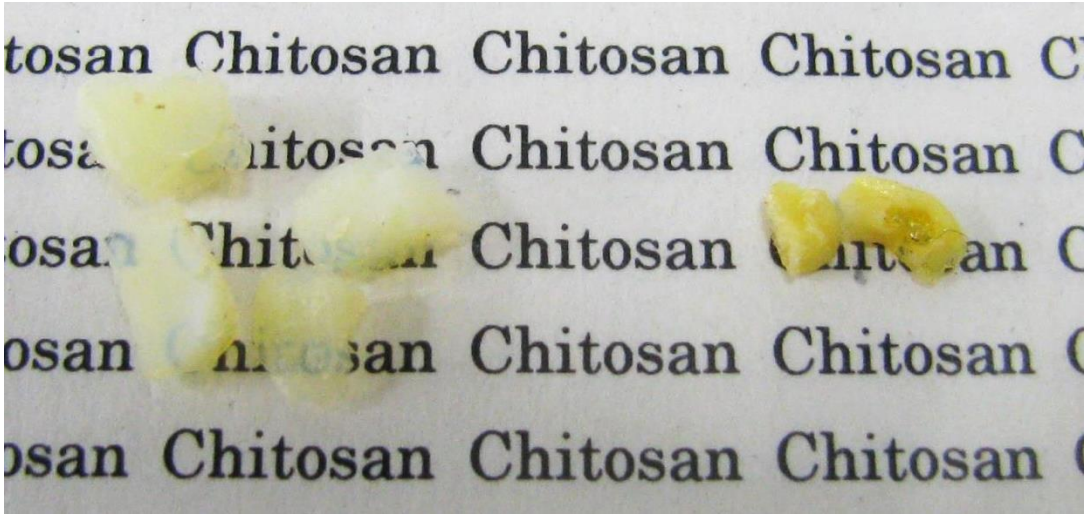

Figure S5. Photographs of unmodified chitosan aerogels before (left) and after (right) the water contact angle measurement. The origin of the yellowish color of the aerogel has not yet been clarified, but it might be related to Maillard reaction during supercritical drying.

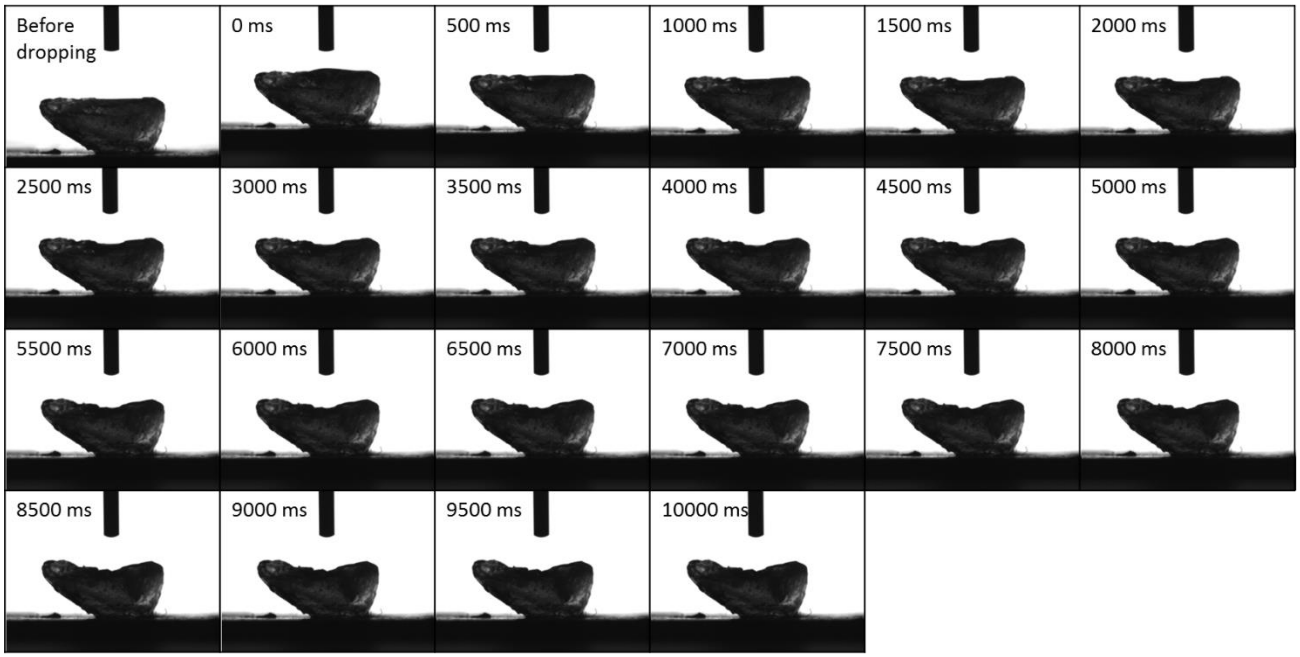

Figure S6. Change in the water droplet on unmodified chitosan aerogel in 10 s after dropping.

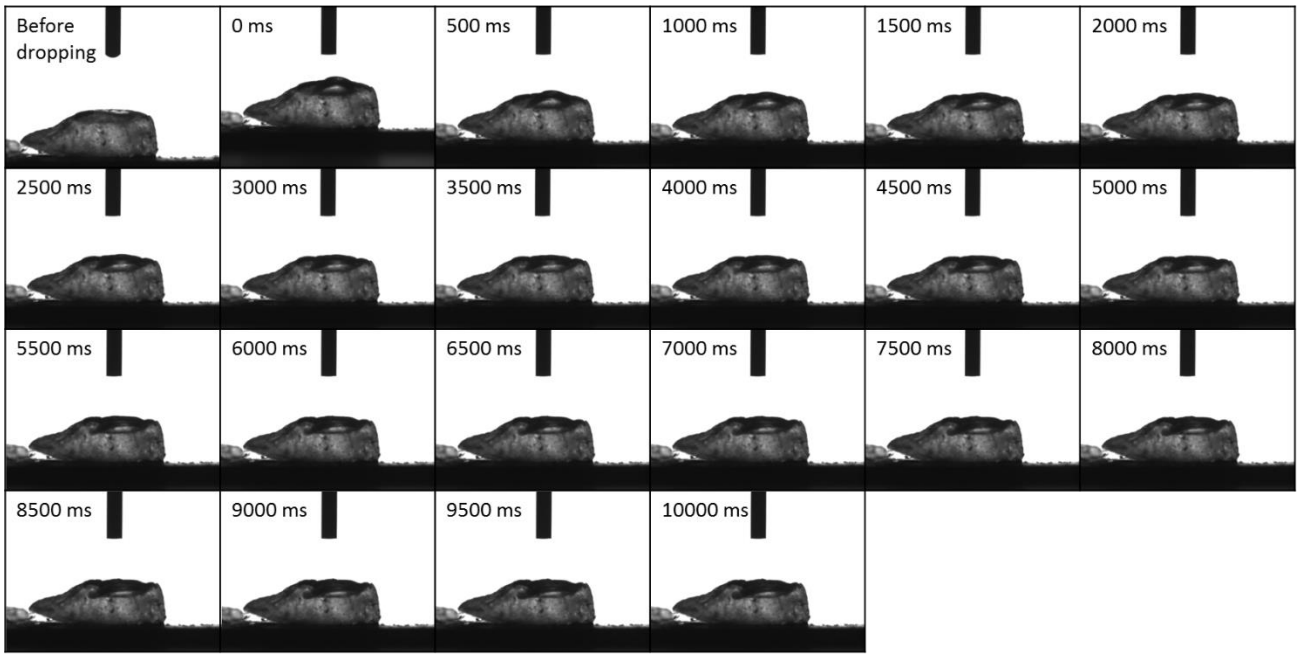

Figure S7. Change in the water droplet on trimethylsilylated (C = 0.1 vol%) chitosan aerogel in 10 s after dropping.

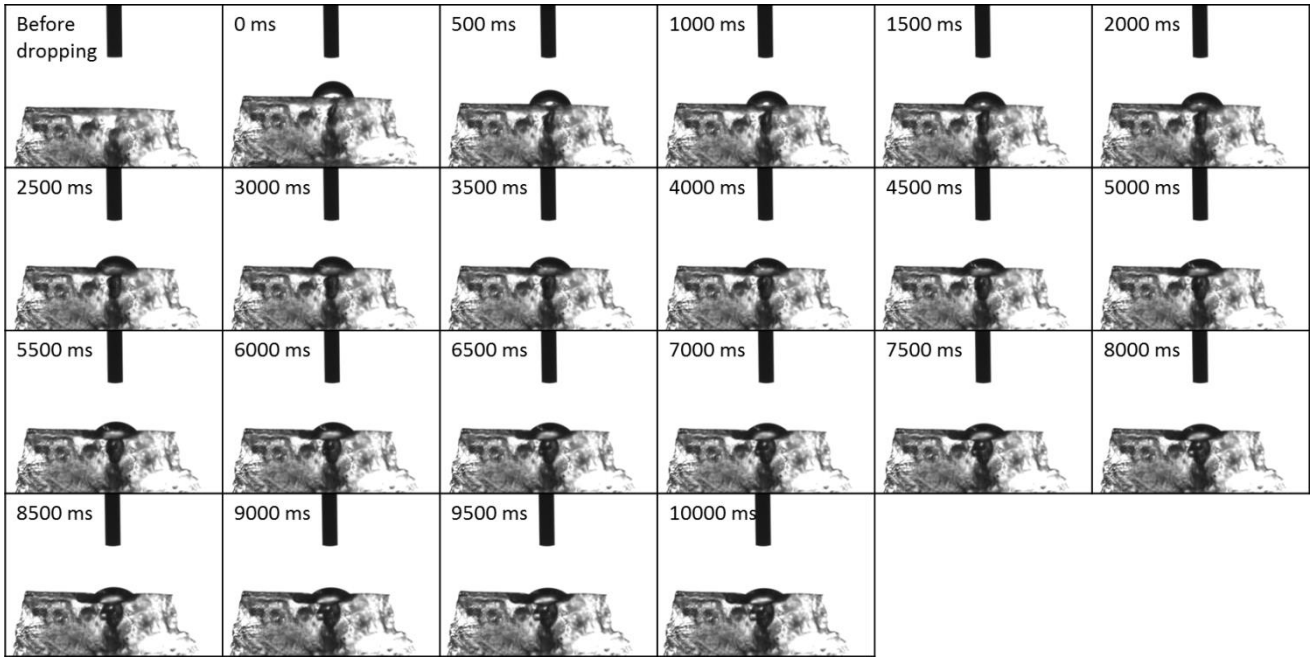

Figure S8. Change in the water droplet on trimethylsilylated (C = 0.2 vol%) chitosan aerogel in 10 s after dropping.

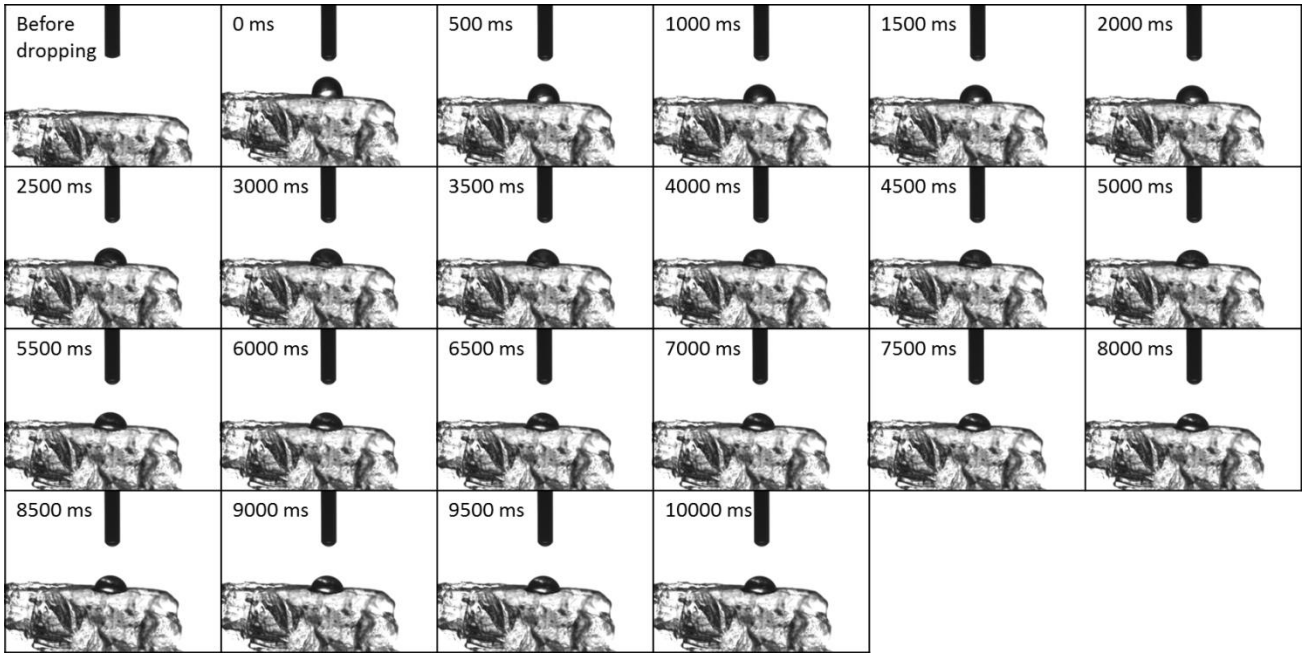

Figure S9. Change in the water droplet on trimethylsilylated (C = 0.25 vol%) chitosan aerogel in 10 s after dropping.

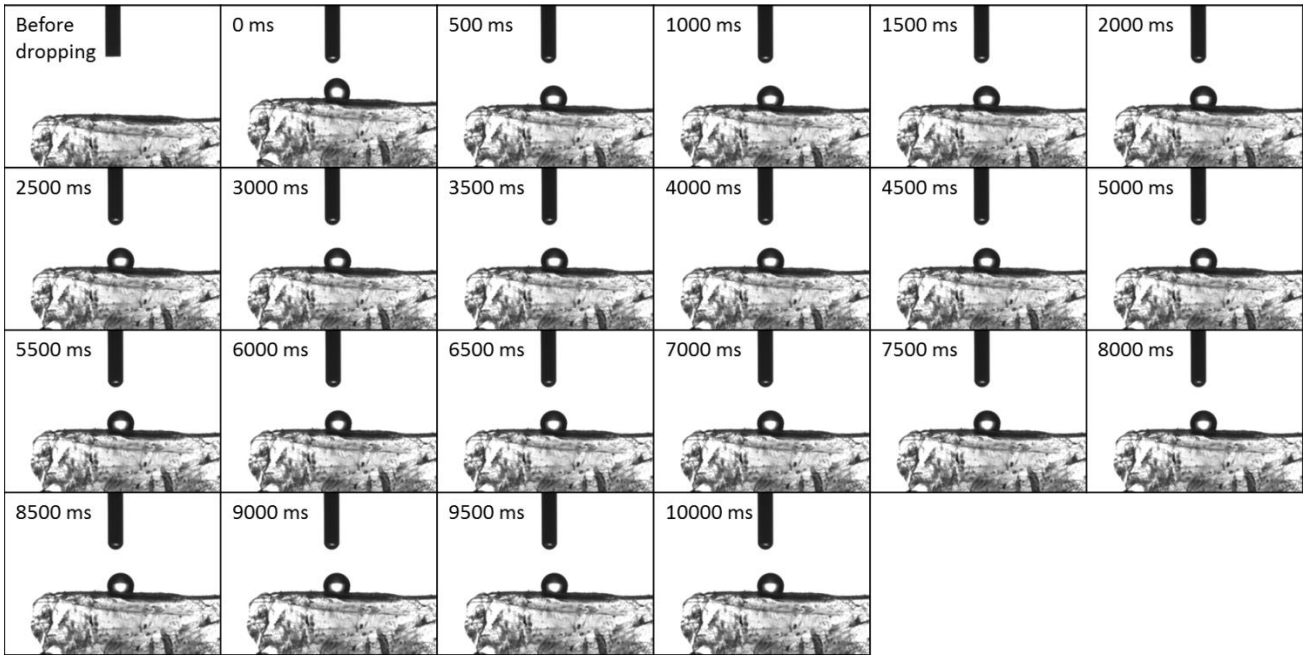

Figure S10. Change in the water droplet on trimethylsilylated (C = 0.35 vol%) chitosan aerogel in 10 s after dropping.

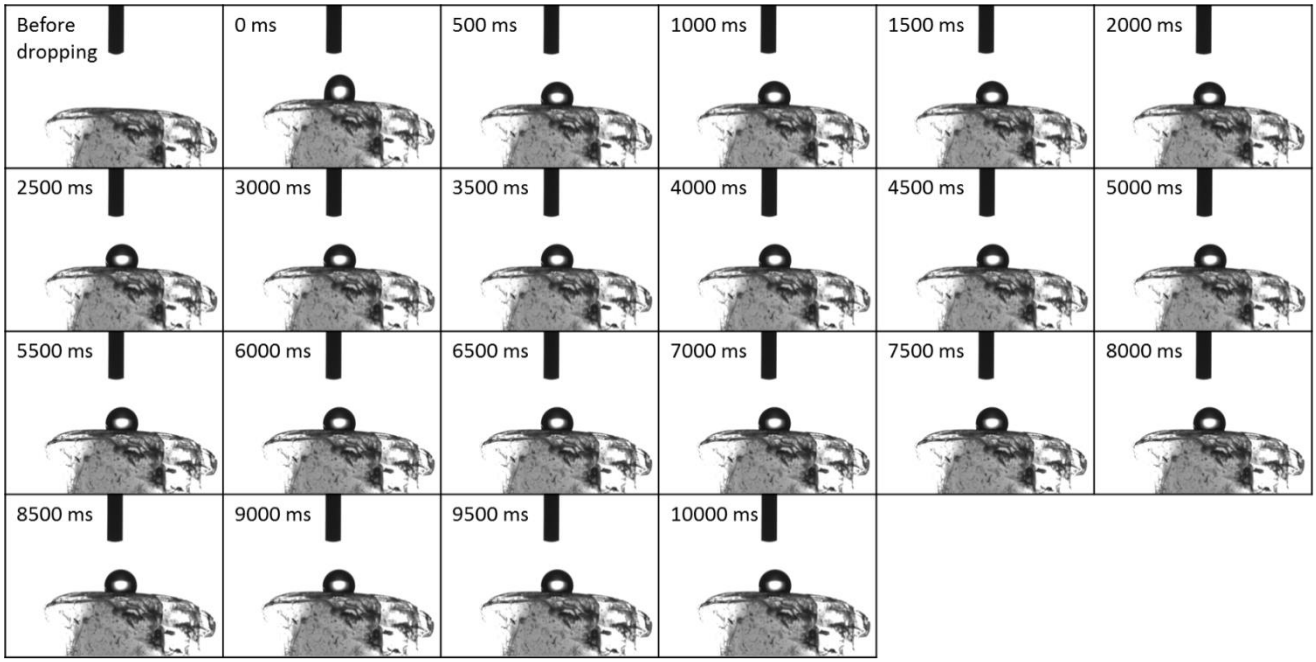

Figure S11. Change in the water droplet on trimethylsilylated (C = 0.5 vol%) chitosan aerogel in 10 s after dropping.

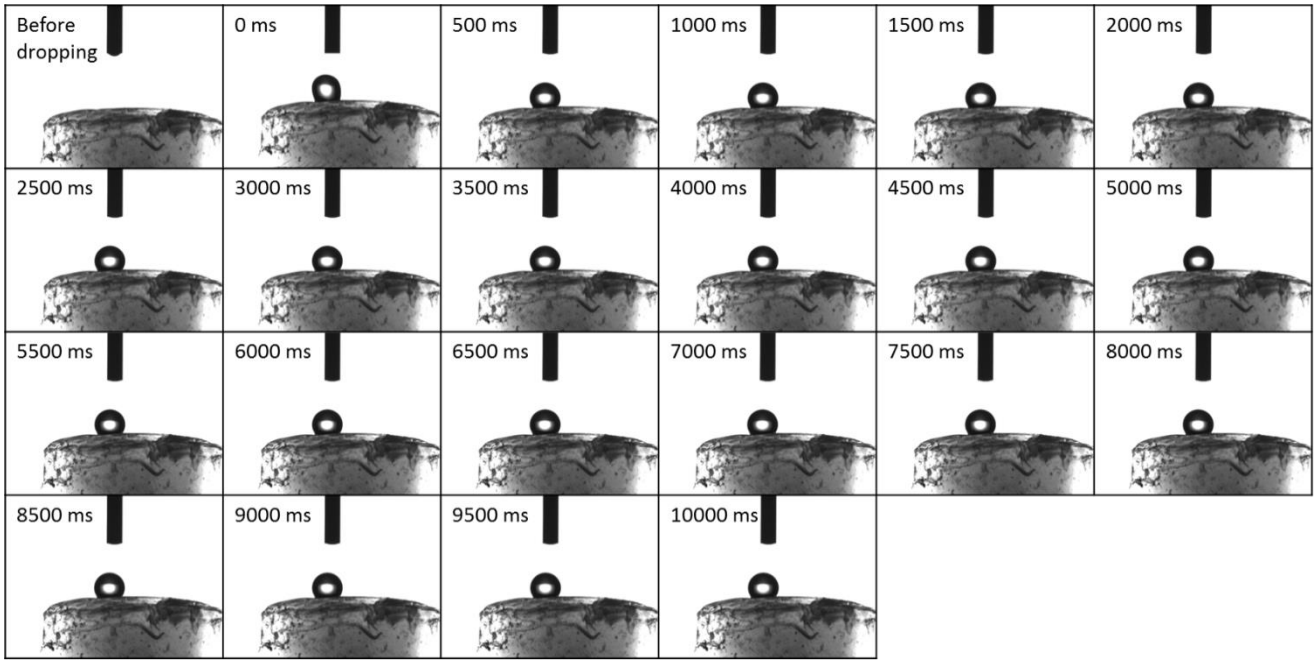

Figure S12. Change in the water droplet on trimethylsilylated (C = 1 vol%) chitosan aerogel in 10 s after dropping.

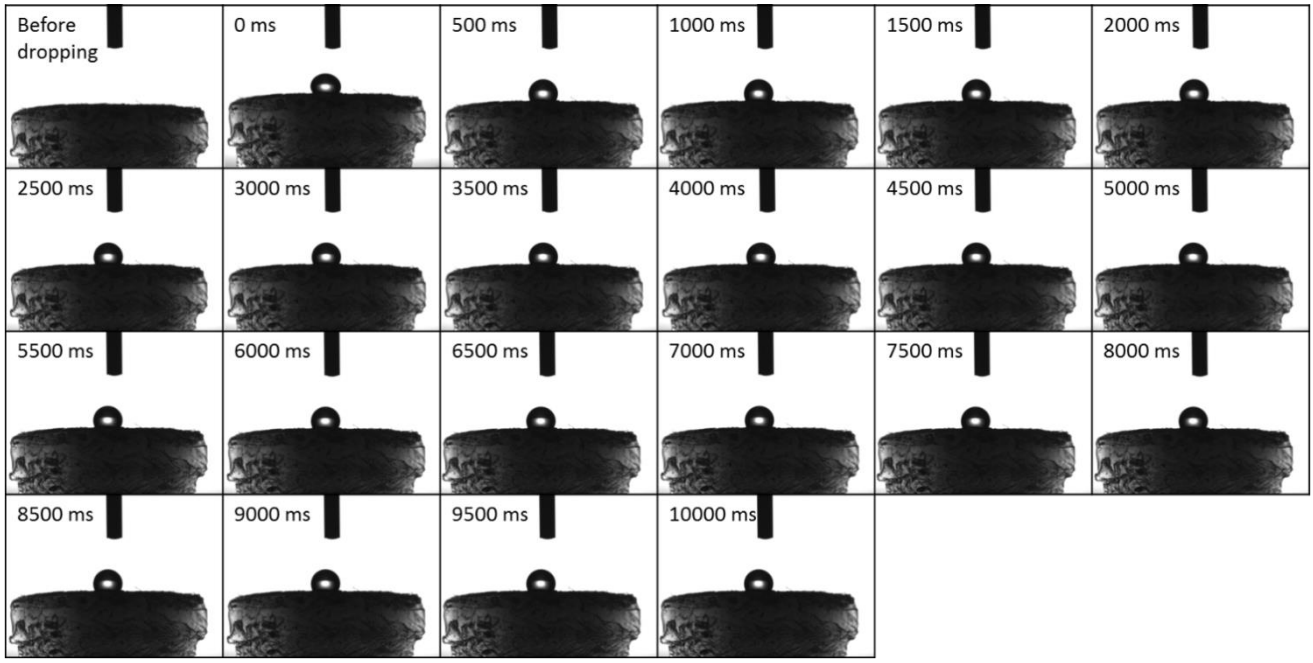

Figure S13. Change in the water droplet on trimethylsilylated (C = 5 vol%) chitosan aerogel in 10 s after dropping.

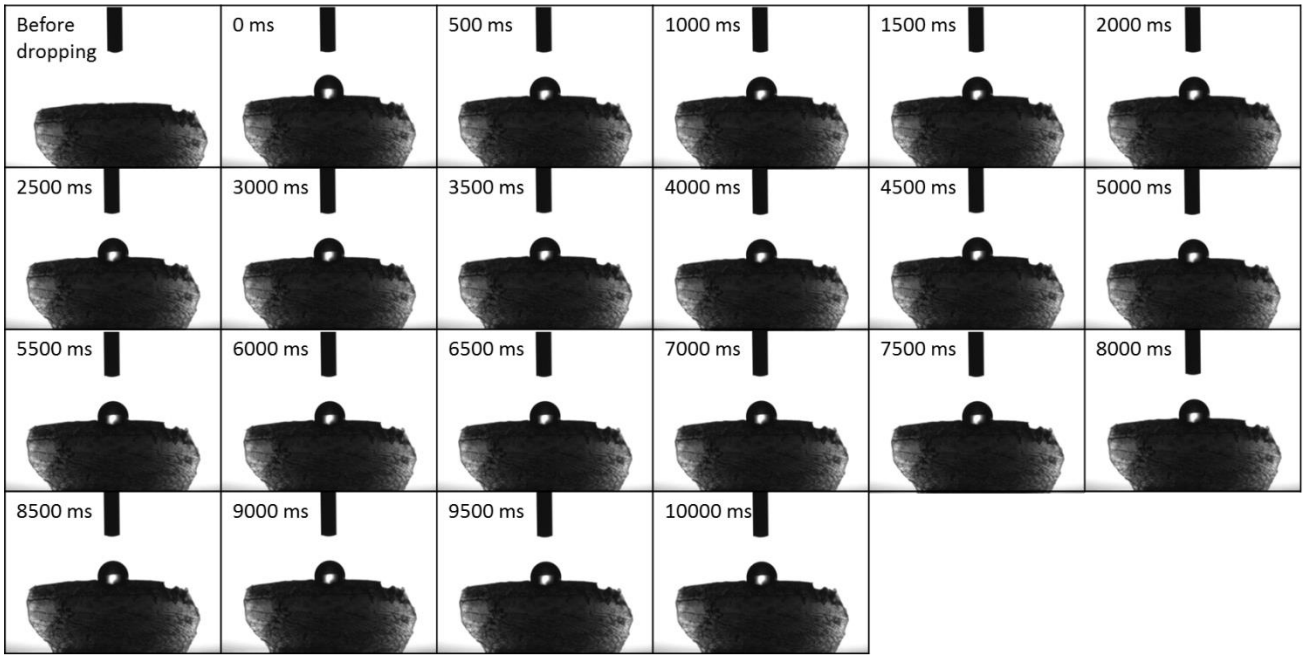

Figure S14. Change in the water droplet on trimethylsilylated (C = 10 vol%) chitosan aerogel in 10 s after dropping.

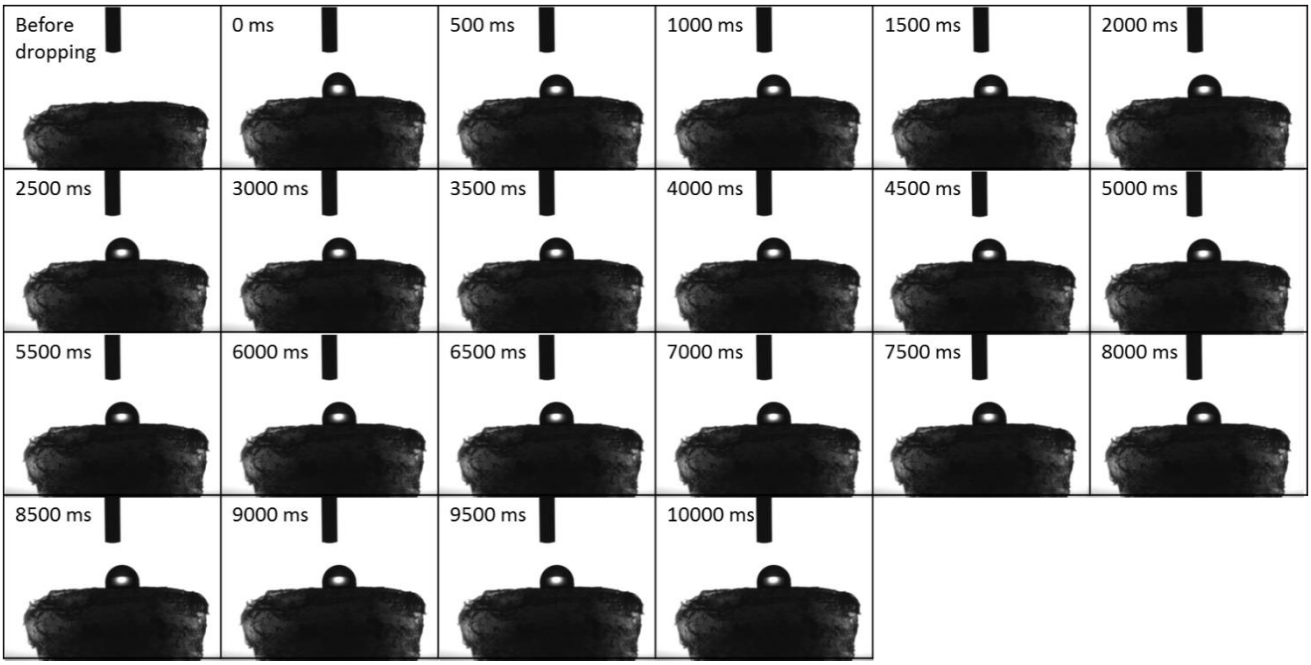

Figure S15. Change in the water droplet on trimethylsilylated (C = 25 vol%) chitosan aerogel in 10 s after dropping.

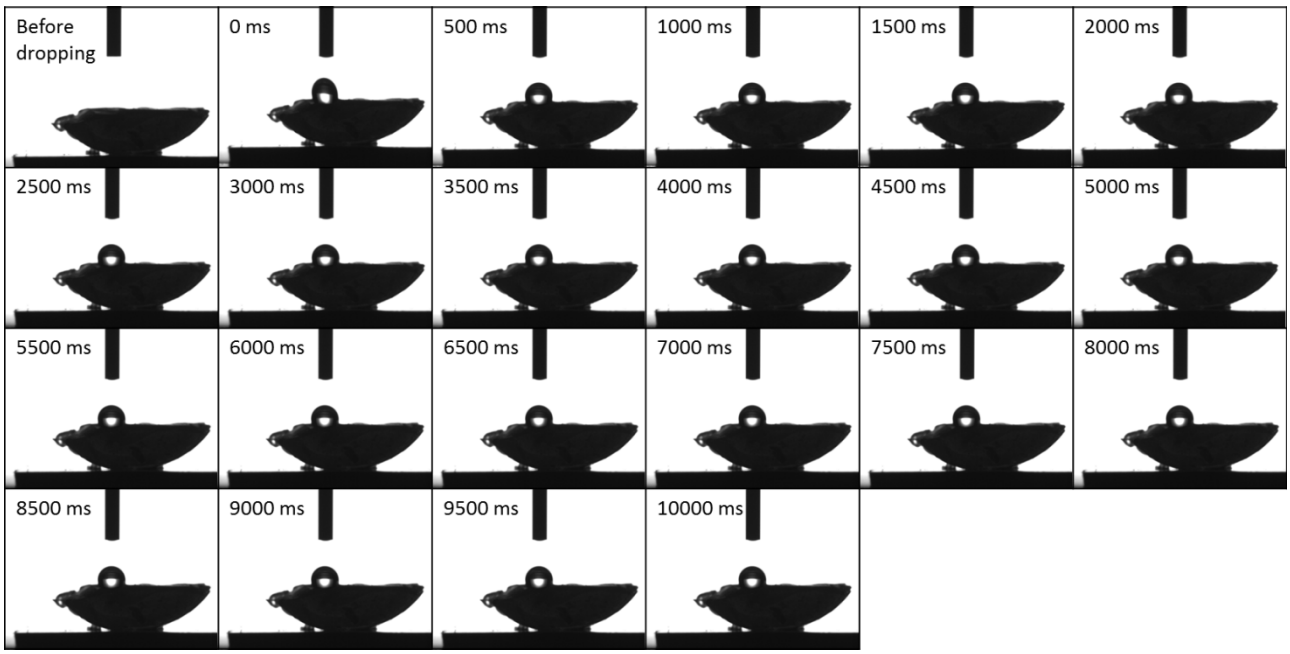

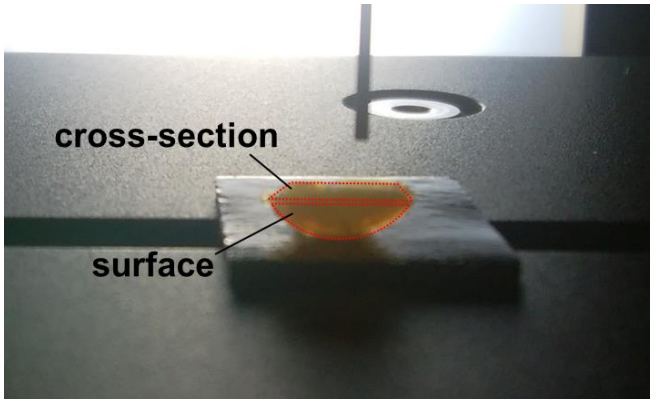

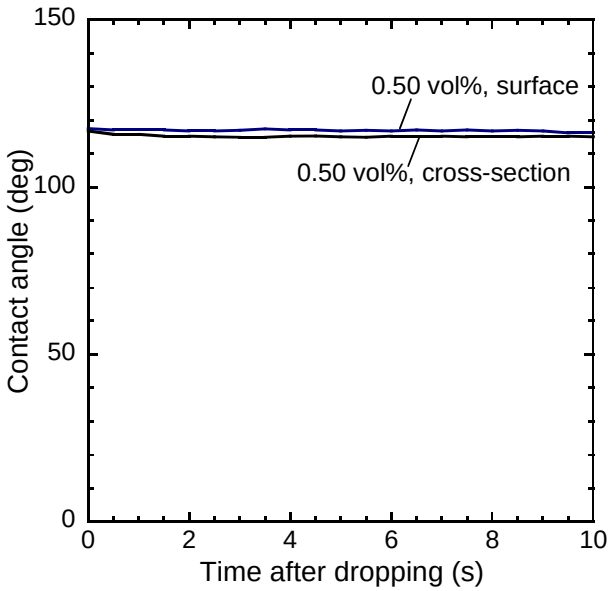

Figure S16. Change in the water droplet on cross-section of trimethylsilylated (C = 0.5 vol%) chitosan aerogel in 10 s after dropping (top). Change in the water contact angles in 10 s after dropping (bottom).

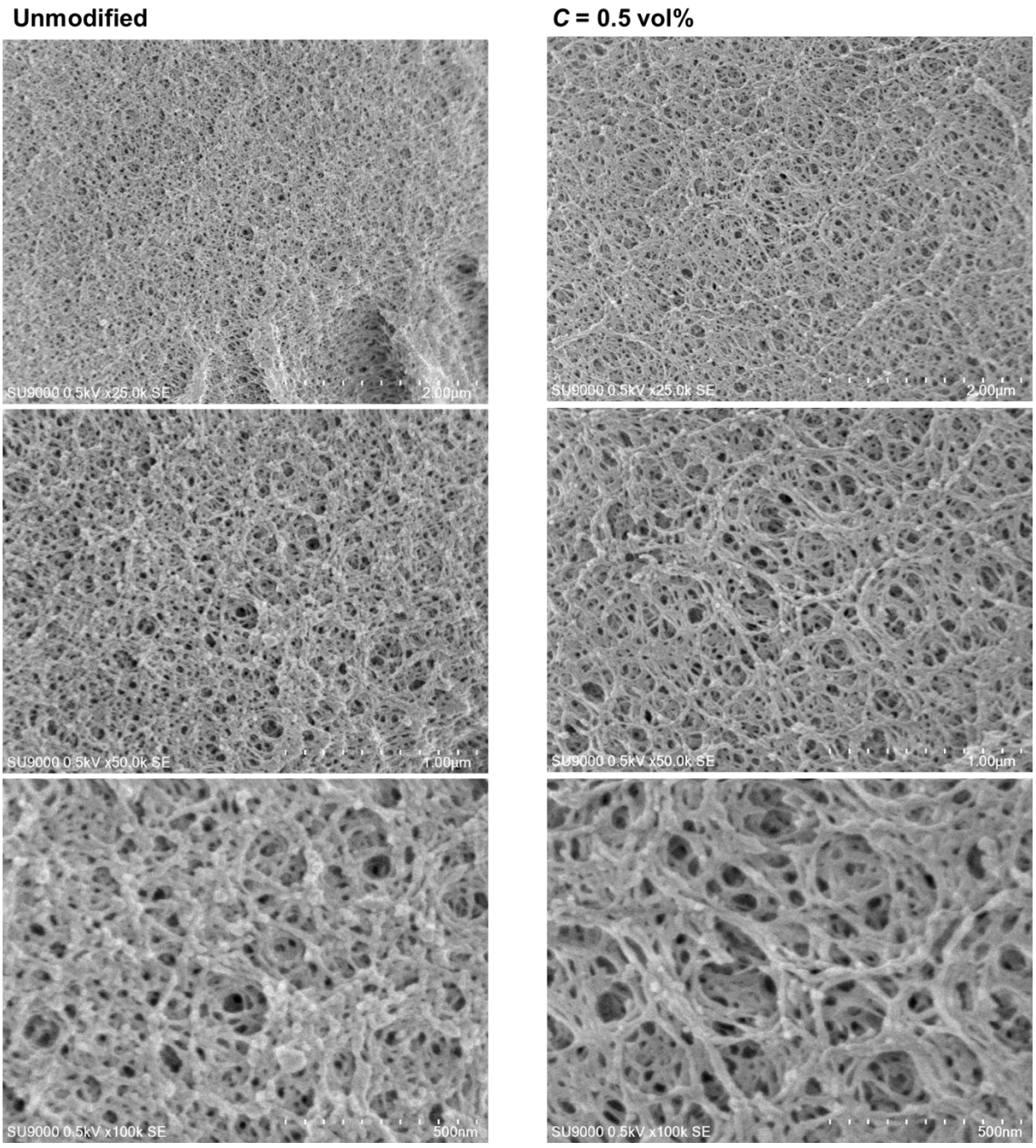

Figure S17. SEM images of unmodified (left) and trimethylsilylated (right) chitosan aerogels.

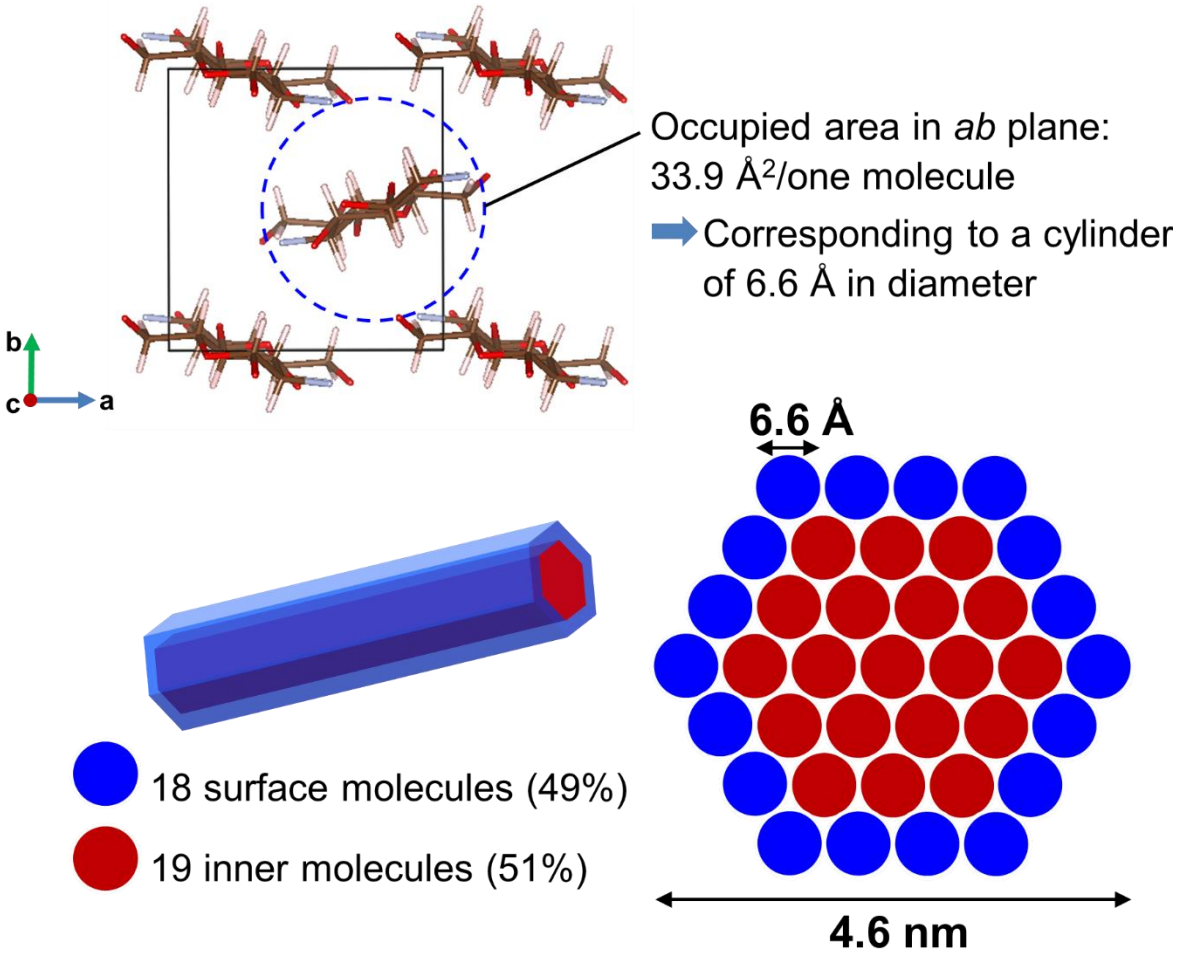

Figure S18. The crystal structure of anhydrous chitosan (top) and a simple estimation for the number of chitosan molecules in one nanofiber (bottom). In the anhydrous crystal of pure chitosan,[S11] one molecule occupies 33.9 Å^2 in the view from *ab* plane, which corresponds to a cylinder of 6.6 Å in diameter. On the basis of hexagonal cylinder approximation, a nanofiber of ~5 nm in diameter contains 37 molecules: 18 at the surface and 19 inside the nanofiber. The occupied area of a molecule may be varied because the actual nanofibers consist of amorphous chitosan regenerated through a cross-linking reaction. We note that this estimation would be reasonable by comparing to crystalline cellulose nanofibers: 36 cellulose molecules in a 3 nm × 5 nm nanofiber.[S12]

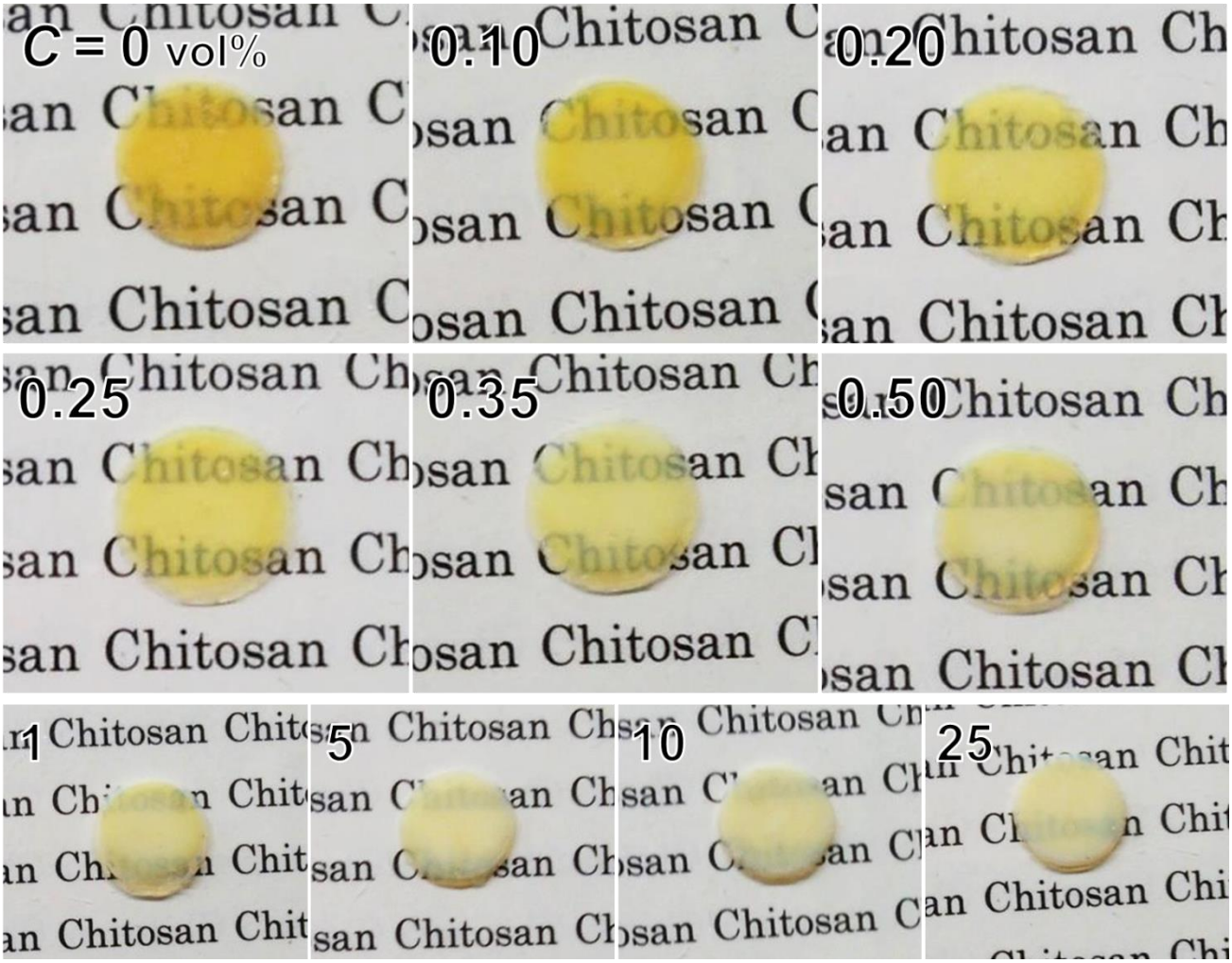

Figure S19. Photographs of the samples after the compression test. The compressed sample bended to some extent by hand (bottom).

Table S3. Dimensions of cylindrical samples for compression test.

HMDS (vol%)	Diameter (mm)	Height (mm)
0	10.4	4.1
0.10	11.1	4.3
0.20	11.4	4.2
0.25	11.9	4.4
0.35	11.8	4.8
0.50	11.2	4.5
1.00	10.9	4.6
5.00	10.2	4.0
10.0	10.2	4.1
25.0	9.9	3.7

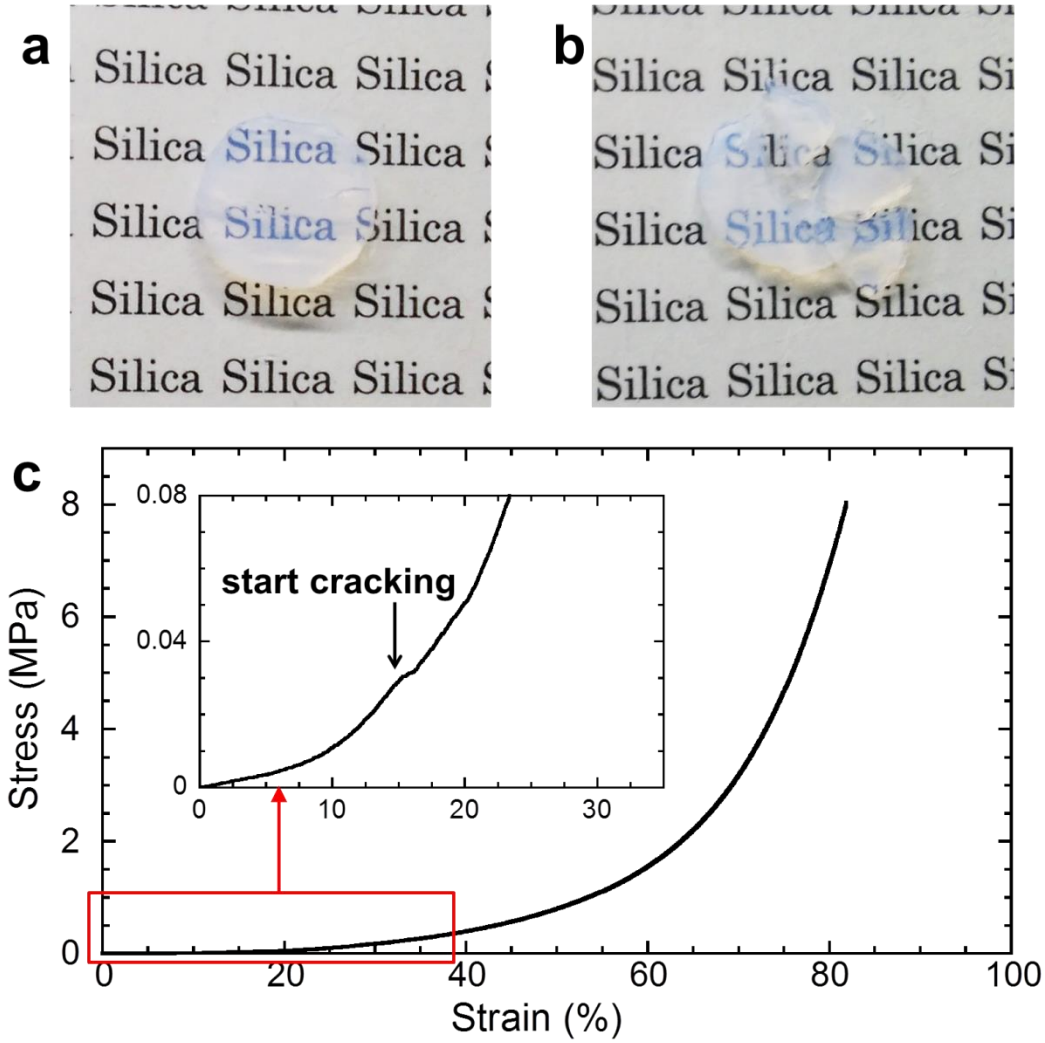

Figure S20. Compression test for conventional silica aerogel (diameter: 12.6 mm, height: 4.3 mm, and apparent density: 0.160 g cm^{-3}). Appearance of the sample a) before and b) after the compression. c) Compression stress–strain curve for the sample. The sample started to crack at the strain of ~15%.

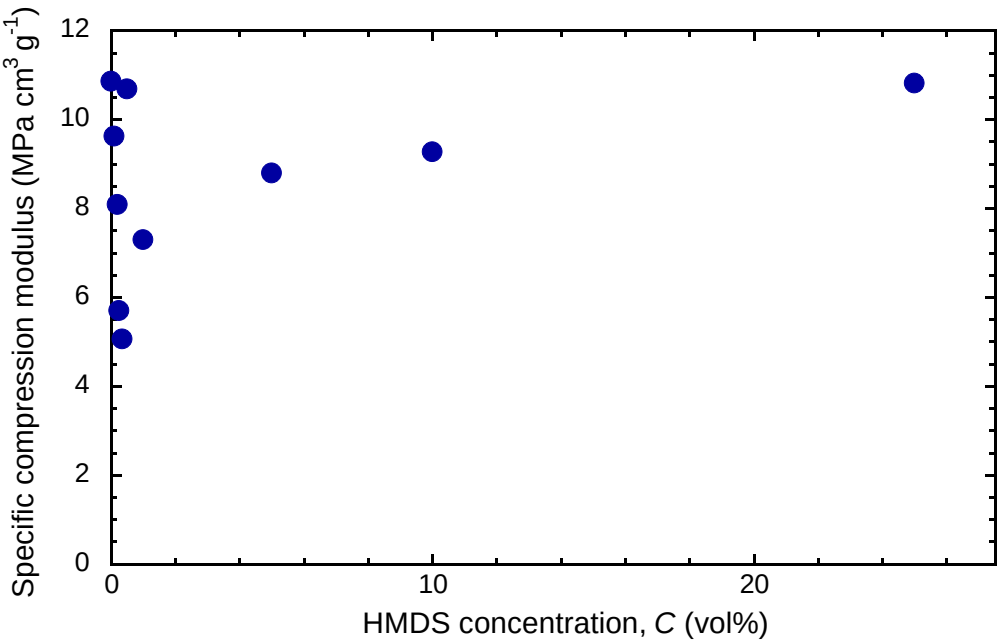

Figure S21. Change in specific compression modulus (elastic modulus divided by apparent density) with HMDS concentration.

Estimation of Thermal Conductivity Components

Thermal conductivity of porous materials, λ_{total}, is the sum of four components:

$$\lambda_{total} = \lambda_{s,cond} + \lambda_{g,cond} + \lambda_{g,conv} + \lambda_{rad} \quad \text{(S2)}$$

where $\lambda_{s,cond}$ is solid-phase conduction, $\lambda_{g,cond}$ is gas-phase conduction, $\lambda_{g,conv}$ is gas convection, and λ_{rad} is radiation. The gas convection, $\lambda_{g,conv}$, is negligible when the pore size is smaller than ~3 mm.[S13] In our case, the radiation, λ_{rad}, is also negligibly small (< ~0.001 W m^{-1} K^{-1}), because λ_{rad} becomes large only at high temperature or when the density is extremely small.[S13] The other two components are calculated by the following equations:

$$\lambda_{s,cond} = (1-\xi)k'\left(\frac{\rho}{\rho_s}\right)^{0.88}\lambda_{s,0} \quad \text{(S3)}$$

$$\lambda_{g,cond} = \xi\frac{\lambda_{g,0}}{1+2aK_n} \quad \text{(S4)}$$

where ξ = 1 – (ρ/ρ_s), ρ and ρ_s are the apparent and solid phase densities, $\lambda_{s,0}$ is the thermal conductivity of pure solid phase, $\lambda_{g,0}$ is the thermal conductivity of pure gas phase, k' and a are the constants, $K_n = \Lambda/\Phi$ is Knudsen number, Λ is the mean free path of the gas molecule, and Φ is the characteristic dimension of pores. By assuming that the nitrogen adsorption measurement reflects the pore structure of the aerogels, we estimated Φ values from BJH plots (Fig. 4d) to be ~58 nm (unmodified aerogel) and ~76 nm (modified aerogel at C = 0.5 vol%). On the basis of this assumption and Λ = 70 nm, a = 1, and $\lambda_{g,0}$ = 0.026 W m^{-1} K^{-1} (values for air),[S14] the HMDS-modified aerogel (C = 0.5 vol%) is expected to have 1.58 and 1.19 times larger $\lambda_{s,cond}$ and $\lambda_{g,cond}$ values, respectively, compared to the unmodified aerogel. These increases in the thermal conductivity components are mainly derived from the increases in apparent density (Fig. S4) and pore size.

The above-mentioned estimation predicts that higher HMDS concentrations would cause an increase in the thermal conductivity up to 1.2–1.6 times compared to the unmodified aerogel. Concerning the potential application for thermal insulators, further work will be needed to unveil the factors controlling the pore structure.

References

[S1] A. Singh, S. S. Narvi, P. K. Dutta and N. D. Pandey, *Bull. Mater. Sci.*, 2006, **29**, 233.

[S2] R. Valentin, B. Bonelli, E. Garrone, F. Di Renzo and F. Quignard, *Biomacromol.*, 2007, **8**, 3646.

[S3] K. Kurita, M. Hirakawa, S. Kikuchi, H. Yamanaka and J. Yang, *Carbohydr. Polym.*, 2004, **56**, 333.

[S4] H. Sai, R. Fu, L. Xing, J. Xiang, Z. Li, F. Li and T. Zhang, *ACS Appl. Mater. Interfaces*, 2015, **7**, 7373.

[S5] J. M. Yang, W. Y. Su, T. L. Leu and M. C. Yang, *J. Membr. Sci.*, 2004, **236**, 39.

[S6] W. Wei, L.-Y. Wang, L. Yuan, Q. Wei, X.-D. Yang, Z.-G. Su and G.-H. Ma, *Adv. Funct. Mater.*, 2007, **17**, 3153.

[S7] A. Philbrook, C. J. Blake, N. Dunlop, C. J. Easton, M. A. Keniry and J. S. Simpson, *Polymer*, 2005, **46**, 2153.

[S8] K. Albert, B. Peters, E. Bayer, U. Treiber and M. Zwilling, *Z. Naturforschung B*, 1986, **41**, 351.

[S9] S. Haukka and A. Root, *J. Phys. Chem.*, 1994, **98**, 1695.

[S10] W. Mormann, *Cellulose*, 2003, **10**, 271.

[S11] P.-K. Naito, Y. Ogawa, D. Sawada, Y. Nishiyama, T. Iwata and M. Wada, *Biopolymers*, 2016, **105**, 361.

[S12] R. J. Moon, A. Martini, J. Nairn, J. Simonsenf and J. Youngblood, *Chem. Soc. Rev.*, 2011, **40**, 3941.

[S13] C. Forest, P. Chaumont, P. Cassagnau, B. Swoboda and P. Sonntag, *Prog. Polym. Sci.*, 2015, **41**, 122.

[S14] *CRC Handbook of Chemistry and Physics, 88th edition*, D. R. Line Ed., CRC Press, New York, 2008, p. 6-200.